

KINETICS AND MECHANISM OF THE CHLORINATION OF FERROCHROMIUM.....

L.R. NELSON Pr.Eng., B.Sc. (Eng), M.Sc. (Eng), M.A.I.M.E.

Pyrometallurgy Division, Council for Mineral Technology, Private Bag X3015, Randburg 2125 South Africa

R.H.ERIC B.Sc. (Eng), M.Sc. (Eng), Ph.D., F.S.A.I.M.M., M.A.I.M.E.

Department of Metallurgy and Materials Engineering, University of the Witwatersrand, 1 Jan Smuts Avenue, Johannesburg 2000 South Africa

Accepted for the Extraction Metallurgy '89 Conference, organized by the Institution of Mining and Metallurgy, and which is to be held in London, on 10 - 13 July, 1989.

SYNOPSIS

The formation of pure chromic chloride as an intermediate to pure chromic oxide and pure chromium metal production was investigated by the chlorination of sintered ferrochromium pellets. Short cylinders of sintered ferrochromium were chlorinated in a furnace at temperatures between 800 and 975°C, the molar fraction of reactant chlorine gas varying between 0.18 and 0.5. The reaction proceeds by a topochemical process, and the ferrochromium exhibits unreacted shrinking-core behaviour, giving rise to a multilayer structure in partly reacted specimens. The major resistance to the overall rate of reaction, at temperatures exceeding 935°C, appears to be the rate of diffusion of product vapours through the layer of product ash. A mathematical model of the rate of reaction is presented.

NOMENCLATURE

Symbol	Description	Dimensions
A_0	Frequency factor	-
b	Stoichiometric coefficient	-
c	Stoichiometric coefficient	-
d	Stoichiometric coefficient	-
E_A	Activation energy	$ML^2t^{-2}n^{-1}$
(g)	Gaseous phase	
ΔG°	Standard free-energy change	$ML^2t^{-2}n^{-1}$
h_p	Heat-transfer coefficient of a particle	$Mt^{-3}T^{-1}$
ΔH°	Standard enthalpy change	$ML^2t^{-2}n^{-1}$
k	Rate constant	Depends on order
$k_{d,ic}$	Rate constant for diffusion control by the ash layer of the product on an infinite cylinder	t^{-1}
$k_{d,s}$	Rate constant for diffusion control by the ash layer of the product on a sphere	t^{-1}
(l)	Liquid phase	
L_{ave}	Average dimension of the pellet	L
m	Mass of the pellet	M
m_0	Initial mass of the pellet	M
m_t	Mass of the pellet at time t	M
m_{Cr}	Mass of contained chromium	M

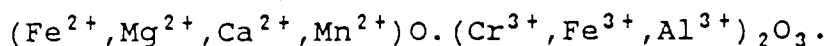
N_{BiH}	Modified Biot number: $h_p L / \lambda_e$	-
p_{Cl_2}	Thermodynamic partial pressure of chlorine gas	-
R	Universal gas constant	$ML^2 t^{-2} T^{-1} n^{-1}$
(s)	Solid phase	-
t	Time	t
T	Temperature	T
T_0	Initial reaction temperature	T
v_{298K}	Linear gas velocity at 298K	Lt^{-1}
X	Fractional conversion	-
x_{Cl_2}	Molar fraction of chlorine gas	-
λ_e	Effective thermal conductivity	$MLt^{-3}T^{-1}$

INTRODUCTION

Conventional routes for the production of chromic oxide and pure chromium metal usually involve the use of soda ash. However, a number of disadvantages are associated with this technology. These include the need for elaborate preparation of the chromite (crushing, drying, and milling to 90 per cent passing 74 μ m), the need for sophisticated equipment and lengthy processes for efficient separation and collection of the products, and the fact that carcinogenic, hexavalent chromium is produced. Chlorination has been successfully used to produce pigment-grade titanium oxide and pure titanium, magnesium, and zirconium metals on an industrial scale. The application of chlorination technology to the production of chromic oxide and chromium metal was therefore considered to be an attractive potential alternative to the conventional soda-ash technology.

The production of pure chromic chloride (CrCl_3) as an intermediate product is necessary for the subsequent production of either chromic oxide or chromium metal. The carbochlorination of chromite was considered to be a suitable route for the production of chromic chloride as early as 1913¹. However, a number of problems are associated with this method.

Naturally occurring chromite has a complex spinel structure, which can be roughly represented by



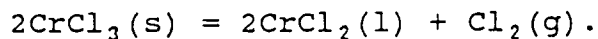
During carbochlorination, the oxidic gangue constituents (comprising about 25 per cent by mass) are converted to metal chloride species, which consume chlorine and reduce the effective volume of the reactor.

Chromite contains magnesium oxide and, to a lesser extent, calcium oxide and manganese oxide, and these oxides form liquid dichloride species at typical chlorinator operating temperatures. These fused chlorides may accumulate to such an extent that they can totally blind the reactor. The presence of silica, which is essentially inert to chlorine at the temperature of the reaction, exacerbates this problem. Furthermore, the high-boiling-point dichloride species still have a considerable vapour pressure (Fig. 1) under the conditions of the reaction, and so have the potential to contaminate the first- condensed, 'pure' chromic chloride product.

The need for a reductant such as petroleum coke, which is expensive in South Africa, is another disadvantage. In particular excessive chlorine-consuming species such as hydrogen and sulphur must not be introduced by the reducing agent.

A most serious problem encountered in the carbochlorination of chromite is the potential for the formation of liquid chromous chloride, instead of chromic chloride, in the reactor, according

to the disproportionation reaction



The presence of liquid chromous chloride is obviously highly undesirable, since it can lead to the blinding of a packed-bed reactor, or the defluidization of a fluidized-bed reactor. Furthermore, the carbon monoxide and carbon dioxide gases produced by the carbochlorination reaction dilute the reactant chlorine gas, which further enhances the potential for the disproportionation reaction to occur in chlorine-depleted zones.

In an effort to overcome some of these problems, Edwards² investigated the chlorination of the next-cheapest chromium-bearing source, namely pre-reduced chromite. The main advantages of this process are that the further addition of carbonaceous reductant is unnecessary, which in turn leads to significantly less gangue material being chlorinated. However, the presence of unchlorinated gangue magnifies the problems associated with the removal of residues from the chlorinator.

Therefore, despite its higher cost, ferrochromium was considered to be the most suitable chromium-bearing source because its use would almost completely eliminate the problems caused by the gangue constituents of chromite. As a result, the operation of the reactor would be greatly simplified and the purity of the chloride product would be enhanced.

An examination of the available literature revealed a dearth of fundamental kinetic data regarding the direct chlorination of solid ferrochromium. Fundamental data pertaining to the selective chlorination of ferrochromium and the chlorination of ferrochromium in molten chloride baths were found, but were not specifically applicable to the proposed process. However, it was interesting to note that the diffusion of chlorine gas through an outer layer of chromium chlorides was claimed to present the chief resistance to the overall rate of chlorination of solid

ferrochromium in both of these cases^{3,4}.

Consequently, the primary objective of the present investigation became the elucidation of the fundamental kinetics and mechanisms of the direct chlorination of ferrochromium. In particular, the rate data were to be generated in a form in which they could be used for the design of a suitable larger-scale chlorinator. Moreover, only aspects of the chlorination step itself were addressed, since the separation of chromic chloride in a fractional condensation stage has already been investigated to a limited extent⁵.

BASIC CHEMISTRY AND THERMODYNAMICS OF THE PROCESS

Ferrochromium can be considered to be a double carbide and silicide of chromium and iron, containing traces of other metallic impurities. At reaction temperatures exceeding 800°C, essentially all the species except carbon and silica, both of which remain 'inert' to chlorination, are chlorinated.

Three chlorides of chromium and three of iron are stable under typical reaction conditions. They are: chromous chloride (CrCl_2), chromic chloride (CrCl_3), chromium tetrachloride (CrCl_4), ferrous chloride (FeCl_2), monomeric ferric chloride (FeCl_3), and dimeric ferric chloride (Fe_2Cl_6). Chromic chloride is the only chromium chloride species that is stable enough to fulfil the requirements of an intermediate product amenable to subsequent processing. Chromous chloride is deliquescent and therefore not easily stored, and chromium tetrachloride is stable in the gaseous state only at elevated temperatures. Moreover, ferric chloride is the desired byproduct, since the differences in physical and physicochemical properties of the trichlorides of chromium and iron allow the efficient vapour-phase separation of 'pure' chromic chloride (Fig. 1). The separation is aided by the apparent non-existence of any double chloride species of iron and chromium.

The possible reactions of chromium and its major carbide phase (represented by Cr_7C_3), and iron and its major silicide phase (represented by Fe_3Si), are all thermodynamically favourable and highly exothermic (Table I). Chromic chloride is the thermodynamically favoured chromium chloride species at reduced temperatures (less than 810°C), while chromium tetrachloride becomes more stable at elevated temperatures. In the case of iron chlorides, dimeric ferric chloride is the thermodynamically favoured species at reduced temperatures, but monomeric ferric chloride becomes increasingly stable at elevated temperatures (three times more⁶ of the monomeric form, by volume, is present at 900°C).

A number of disproportionation reactions are possible for chromium and iron chlorides (Table I). In order that the formation of liquid chromous chloride by thermal dissociation of chromic chloride in the reactor (reaction 18) can be avoided, yet concurrently the maximum possible efficiency of chlorine utilization can be maintained, the partial pressure of chlorine must be maintained⁶ above 7.48×10^{-4} atmospheres at 1000°C . However, Maier⁵ claimed that this amount of chlorine, over and above the stoichiometric quantity required for the production of chromic chloride, is not sufficient because a portion of the chlorine is consumed immediately in the production of chromium tetrachloride (reaction 17). Therefore, the dissociation pressure of chromic chloride must be maintained by the addition of enough excess chlorine to ensure that the maximum thermodynamic quantity of chromium tetrachloride is formed, namely 6.42×10^{-2} atm of chromium tetrachloride at 1000°C .

The disproportionation reactions of ferric chloride (reactions 20 and 21) also produce undesirable liquid ferrous chloride, and the partial pressure of chlorine must be maintained above 0,125 atm to prevent this reaction occurring⁶. However, the disproportionation reaction of ferric chloride also makes it a

potentially important chlorinating agent in chlorine-depleted zones (reaction 10)

EXPERIMENTAL PROCEDURE

Single-particle experiments were chosen for the fundamental study of the chlorination reaction, because only by this method could the reaction conditions be controlled with sufficient precision for the mechanism to be determined. The main technique used was thermogravimetric analysis (TGA). Chemical analysis, mineralogical examination by scanning electron microscopy (SEM) with energy-dispersive spectroscopy (EDS) and X-ray mapping (XRM), and X-ray diffractometry (XRD) of the chlorinated product residue were used to further clarify the reaction mechanism.

Materials

Typical charge-chrome (high-carbon-ferrochromium) fines were obtained from a local producer of ferrochromium, but the individual lumps were found to be too unhomogeneous for reproducible results to be obtained from single-particle experiments. Consequently, short cylinders of ferrochromium were manufactured for the testwork. These cylinders had an average dimension of 13.98 mm (a length-to-diameter ratio of 1.062), an average mass of 13.811 g, and an average porosity of 8.97 per cent.

The chemical analysis of these pellets was almost identical to that of the bulk charge-chrome sample (Table II). XRM showed that the chromium-iron carbide and silicide contents of a typical pellet (Fig. 2) were about 76 and 17 per cent (by area) respectively. Uniformly distributed, closed, spherical pores (less than 50 μ m in diameter) accounted for the remaining 7 per cent by area. About 70 per cent of the pores were found to contain inclusions of slag, mainly silica and fayalite, which had been introduced by the sintering process. The sintered pellets

were also found to possess a thin oxide coating about 5 μ m in thickness. Consequently, this layer was removed by bead-blasting, light polishing with silicon carbide paper, and washing with acetone just prior to chlorination.

'Dry' chlorine gas (with a stated purity of 99.6 per cent) was supplied in cylinders by Sappi Ltd. High-purity nitrogen gas with claimed water and oxygen contents of less than 10 p.p.m. each, was supplied in cylinders by Afrox Ltd. Nitrogen gas served the dual functions of protecting the balance from the hot corrosive environment of the reaction and acting as an 'inert' diluent gas for control of the molar fraction of chlorine gas in the reactor.

Apparatus

The chlorination apparatus was designed to provide reliable continuous TGA data for a single pellet of ferrochromium suspended in a chlorine-gas environment, in the temperature range 800 to 975°C. The apparatus (Fig. 3) consisted of the following major components.

Gas supply and purification. Chlorine gas was purified by means of a silica-gel trap and a concentrated (98 per cent) sulphuric acid bubbler. The nitrogen gas was purified by means of a silica-gel trap, a calcium chloride drying tower, a phosphorus pentoxide drying tower, a copper deoxidation furnace operated at 400°C, and a concentrated (98 per cent) sulphuric acid bubbler. Calibrated rotameters(11) were used to meter the purified chlorine and nitrogen gases. The errors in the combined total gas flowrate and the resultant molar fraction of chlorine (x_{Cl_2}) were always less than 3 per cent.

Furnace and mass measurement. An electronic balance(14) was mounted over a movable furnace (15), the vertical movement of which was facilitated by the use of two guide-rollers and four

counterweights placed symmetrically around the furnace shell. A Mettler PM460 balance provided a continuous record of the mass of a single ferrochromium sample, which was held in a quartz basket (30 mm wide and 20 mm high) suspended from the balance by means of a metal hook and a silica suspension fibre (2 mm outer diameter). The accuracy of the balance was greater than 99.9 per cent throughout the course of the reaction.

The balance was housed at ambient temperature in a sealed balance box, which was purged with purified nitrogen gas to protect the instrument from the hot, corrosive environment of the furnace. The nitrogen gas was admitted to the reaction tube (43 mm internal diameter) via a metal baffle(18) and a flow-constriction device(19), and chlorine gas was admitted below the flow-constriction device. This arrangement provided about 0.5 m of reaction tube in which the gases could mix before contacting the ferrochromium sample.

The suspended sample was heated externally by an electrical resistance furnace(15) with a dual winding. This facilitated independent control of the temperature of the sample (800 to 975°C), and provided a high constant temperature (higher than 900°C), which prevented the base of the reaction tube from becoming clogged with product chlorides.

Kanthal A-1 wire (1.2 mm in diameter) was used for the furnace windings, which were driven by separate thyristor power packs (28). The temperatures of the two windings were measured by R-type thermocouples, and were controlled to within 2°C of specified isothermal set points by proportional integral-derivative (PID) controllers(29). The K-type thermocouple, protected from the corrosive chlorine environment by a quartz sheath (5 mm outer diameter), was placed inside the reaction tube adjacent to the sample basket. This 'near-pellet' thermocouple measured the initial temperature of the pellet to within less than 7.5°C, which was considered acceptable in comparison with

the uncertainties in the measurement of the 'true' temperature of the pellet that were caused by its exothermic temperature rise!

Product collection and gas scrubbing. The majority of the metal chloride vapours produced were swept through the widened base of the reaction tube and into a large, air-cooled glass condenser filled with glass wool(32). Uncondensed gases were then vented to a countercurrent, packed-column scrubber(33) of 75 mm diameter and 1 m length, where they were sprayed with a solution of soda ash at a rate of 10 l.min⁻¹. Scrubbed gases emanating from the top of the column were finally exhausted to a fume hood.

Data logging and processing. The mass of the pellet and the temperature measured by the K-type thermocouple were monitored continuously and recorded on a tape data-logging system(40). The fractional conversion of the pellet was then calculated from these data by use of the expression

$$X = \frac{m_0 (1-0.069) - [m_t - m_0(0,069)]}{m_0 (1-0,069)}$$

(The carbon content of each pellet was assumed to be 6.9 per cent by mass, and inert.) The fractional conversion of the pellet was plotted versus reaction time, and the rate of conversion was then calculated by use of the relationship

$$\frac{dX}{dt} = \frac{60}{m_0} \times \frac{d(\Delta m_t)}{dt}$$

Standard experimental procedure

The silica basket was freely suspended from the balance, and the system was allowed to attain thermal equilibrium under the standard flowrate of nitrogen gas (2239 cm³ min⁻¹). The balance was then zeroed by taring, after which the reactor was re-opened

and the silica basket removed. A polished ferrochromium pellet was then weighed on a separate balance, and its principal dimensions were measured with vernier calipers. The pellet was then carefully positioned in the centre of the basket, and the sample and basket were freely suspended from the balance. The furnace was moved into position rapidly so that the sample was placed precisely in the uniform hot zone of the furnace. The reactor was then sealed and allowed to equilibrate for 30 minutes.

Before the reaction was started, chlorine gas was passed through the reaction by-pass line at the required flowrate (usually $1054 \text{ cm}^3 \text{ min}^{-1}$) for 10 minutes. The reaction was then initiated by the admission of chlorine gas directly to the reactor. The mass and temperature of the pellet were carefully monitored during the course of the reaction. After the desired reaction time, the supply of chlorine gas to the furnace was turned off and the furnace was switched off. The pellet was then allowed to cool to below 400°C in an atmosphere of purified nitrogen gas before being removed from the reactor.

After it had been removed, the pellet was immediately weighed on a separate balance, and its principal dimensions were measured with vernier calipers. The pellet was then sectioned, and the thickness and form of the product layers were noted. Samples of the different product layers were stored separately in a dessicator before being submitted for chemical analysis, mineralogical examination, and determination of pore size, pore-size distribution, and density.

Modified experimental procedure

The standard procedure was modified to allow the 'true' temperature at the centre of the pellet to be monitored during chlorination. This was achieved by the use of a spark-eroded pellet, which was placed over the end of a silica thermocouple sheath with an outer diameter of 4 mm. A modified sample basket,

connected to the thermocouple sheath, and with dimensions similar to those of the standard basket, was used. The gap between the thermocouple sheath and the pellet was plugged with silica wool. A K-type thermocouple of diameter 1.0 mm was placed in the thermocouple sheath and positioned at the centre of the pellet.

RESULTS

The short sintered cylinders of ferrochromium were found to be suitable for the simulation of the chlorination of raw ferrochromium. Although the sintering caused a thin oxidized layer to form on the surface of the pellet, the effect of this layer on the overall rate of reaction was found to be negligible, particularly if the pellet was polished and cleaned prior to reaction. Sintered pellets and similar-sized lumps of raw ferrochromium, chlorinated at similar rates, displayed unreacted shrinking-core (USC) behaviour, with a topochemical reaction resulting in multiple layers of product and reactant (Fig. 4). In particular, the ferrochromium core was found to be non-porous, and to form a sharp reaction interface in both types of sample.

Boundary layer mass-transfer effects

The linear gas velocity, calculated at 298K (V_{298K}), was varied between 1 and 5 cm s⁻¹ so that its effects on the rate of chlorination at an initial reaction temperature of 925°C could be established. At gas velocities of 1 and 2 cm s⁻¹, there was an initial 'induction' period, during which no appreciable fractional conversion of the pellet was measured. This was ascribed to reagent-gas starvation, which was thought to occur because the product chloride vapours were not being transported from the reaction interface as rapidly as they formed.

At linear gas velocities greater than 3 cm s⁻¹, the fractional conversions of pellets were identical, which indicated that 3 cm s⁻¹ represented the minimum critical gas velocity.

Consequently, all further testwork was conducted at a linear gas velocity of 4 cm s^{-1} to ensure that reagent-gas starvation and boundary layer mass-transfer effects had a negligible influence on the rate of reaction.

Pellet temperature

The chlorination reactions of ferrochromium are extremely exothermic (Table I). Consequently, convective (and possibly radiative) heat transfer between the gas stream and the surface of the solid particle, and conductive heat transfer within the reacting pellet, must be included into any expression of the overall rate of reaction. Szekely *et al.*⁷ claimed that convective (and radiative) heat transfer provide the major resistance to the energy transfer from the pellet, provided that the modified Biot number, N_{BiH} , is less than 0.2.

N_{BiH} was calculated to be 1.5×10^{-2} at the onset of chlorination, which implies that conductive heat transfer within the pellet provides a negligible resistance to the overall rate of reaction. Under such conditions, negligible temperature gradients exist, and the pellet can be assumed to possess a uniform temperature. The single thermocouple in the centre of the pellet therefore provides measurements of the 'true' temperatures at the centre of the pellet, the reaction interface, and the surface of the pellet.

Two in-pellet thermocouple tests were carried out under standard test conditions ($T_0 = 925^\circ\text{C}$ and $x_{\text{Cl}_2} = 0,32$). Marked temperature rises of up to 68°C after $5\frac{1}{2}$ minutes of reaction were observed, which clearly demonstrate the exothermic nature of the reaction (Fig. 5). Thereafter, the temperature of the pellet decreased during the course of the reaction. It is therefore clear that isothermal conditions did not prevail during the testwork, and that only the initial temperature of the pellet could be defined with any accuracy. Furthermore, the use of a single in-pellet

thermocouple could provide, at best only, a measure of the average temperature of the pellet. Local temperatures could well have exceeded the average temperature, and in fact a maximum pellet temperature of $972,5^{\circ}\text{C}$ was predicted under the experimental conditions employed⁶. Consequently, the reaction temperature was defined as the initial reaction temperature, although cognisance was always taken of the rise in temperature of the pellets.

In tests that were carried out at a lower initial reaction temperature of 800°C , a curious secondary rise in temperature took place after 40 minutes of reaction (Fig. 5). All the pellets that were reacted at 800°C developed a surface layer that cracked after about 40 minutes of reaction. The enthalpy of reaction is essentially independent of temperature, so that the rise in the temperature of the pellet is largely a function of the rate of reaction. It appears that the cracks in the pellet reduced the diffusion distances, thereby enhancing the rate of reaction and so causing the secondary temperature rise.

Effect of particle size

Pellets of three different sizes, with average dimensions (L_{ave}) of 13.7, 10.6, and 7.3 mm, were used in the tests. The smaller pellets were produced by the removal of the product ash layer of partly reacted pellets, and repolishing of the ferrochromium core. The pellets were then chlorinated under standard conditions, and their rates of conversion were calculated by the standard method.

The removal of the layer of product ash to produce the smaller pellets dramatically enhanced the rate of reaction (Fig. 6). This clearly indicates that the rate of chemical reaction at the interface did not provide the dominant resistance to the overall rate of reaction. Furthermore, the curves of fractional conversion versus reaction time were not linear, which shows that

boundary layer mass transfer did not, as expected, have any appreciable effect on the rate of reduction.

The rate of reaction became progressively slower with time, which is entirely consistent with an increasing resistance to diffusion through a layer of product ash that increases in thickness in the course of conversion. It was therefore concluded that diffusion through the product ash layer provides the major resistance to the overall rate of reaction.

Effects of initial reaction temperature

Fig. 7 presents the results of tests that were carried out under standard conditions of $x_{Cl_2} = 0.32$, but with different initial reaction temperatures.

800°C regime. Pellets that were chlorinated at an initial reaction temperature of 800°C reacted faster than those that were chlorinated at initial temperatures between 850 and 900°C. The extremely close correlation between the results of the two tests at an initial temperature of 800°C clearly demonstrate the precision of the experimental technique, and hence the enhanced rate of reaction has to be considered a real effect.

Cracking was found to occur in all the pellets that were chlorinated at an initial temperature of 800°C, which explains this seemingly anomolous result. Obviously the rupture of the surface layer of product ash would reduce the diffusion distance, and thus enhance the rates of reaction. Furthermore, the rate of reaction was enhanced within the first hour of chlorination, coinciding with the time of the secondary temperature rise.

The rupture appeared to be caused by mineralogical changes on the outside of the pellet. The pellets that were chlorinated at an initial temperature of 800°C all developed a hard thin 'skin'. Qualitative analysis by SEM and EDS revealed that this skin

contained an unusual concentration of chlorides and oxides of silica and iron. As reaction progressed, the slight difference in volume between the unreacted ferrochromium and the carbonaceous layer of product ash apparently caused a build up of stress in the skin layer, which eventually resulted in its longitudinal rupture.

850 to 900°C regime. In this temperature regime, the reaction rate appeared to show little, if any, dependence on the initial reaction temperature. It was postulated that the temperatures of the pellets reacted in this regime rarely exceeded the sublimation temperature of chromic chloride (947°C). This would have resulted in the formation of a thick layer of chromic chloride at the reaction interface, and the rate of sublimation of this layer would have been fairly independent of the initial reaction temperature.

Temperatures higher than 900°C. The rate of chlorination of pellets at initial reaction temperatures above 900°C showed a marked dependence on the initial reaction temperature. The reason postulated for this is that, in this temperature regime, the temperatures at the reaction interface were well in excess of the sublimation temperature of chromic chloride (947°C). The rate of sublimation of chromic chloride no longer provided the dominant control of the overall rate of reaction, which would have reassumed its dependence on the initial reaction temperature.

Rate of volatilization of chromic chloride

The theoretical maximum rate of volatilization of chromic chloride, either as $\text{CrCl}_3(\text{g})$, or as the reaction product $\text{CrCl}_4(\text{g})$ was established as follows. Two cold, cylindrical pellets of pure chromic chloride were reacted at initial reaction temperatures of 858 and 931°C (at an x_{Cl_2} value of 0.32). Chromium units in the standard ferrochromium pellets were assumed

to undergo chlorination at the same average rate as the ferrochromium pellet itself, thus allowing the maximum initial rate of chlorination to be compared with the maximum initial rate of volatilization of chromic chloride (Table III).

At low initial reaction temperatures (about 850°C), the rates of chlorination and volatilization were similar. The rate of sublimation of chromic chloride was therefore certain to have provided a significant resistance to the overall rate of reaction. However, the rate of sublimation of pure chromic chloride at an initial temperature of 931°C was almost twice that at 858°C, and almost 1.6 times the corresponding initial rate of chlorination of ferrochromium. This implies that the relative effect of the rate of volatilization of chromic chloride on the overall rate of reaction is reduced dramatically at the higher temperature, probably because the exothermicity of the reaction causes the temperature of the reacting pellet to exceed the sublimation point of chromic chloride (947°C).

Effect of chlorine concentration

Higher concentrations of chlorine increased the rate of chlorination dramatically. An increase in the molar fraction of chlorine from 0.18 to 0.5 reduced the time needed to reach complete conversion from 5½ to 3½ hours (Fig. 8). However, the temperature rise of the pellet was increased markedly (from 54 to 100°C) by the higher concentration of chlorine (Fig. 9). Dilution of the reactant chlorine gas by 'inert' nitrogen gas clearly reduces the exothermicity of the reaction.

PROPOSED REACTION MECHANISM

Because of the impervious nature of the solid ferrochromium reactant the reactant-product interface was sharp. The unreacted alloy surface was considered to consist predominantly of a mixture of chromium carbide, $(Cr,Fe)_7C_3$, and iron silicide

(approximated by Fe_3Si) phases (Fig. 10). The reaction chlorinated both of these phases. However, the chlorination of iron silicide was more thermodynamically favourable (Table I), and was accompanied by the rapid transport of the product chloride vapours, whereas the chlorination of the chromium carbide resulted in the formation of a solid mixture of graphite and a large proportion of unvolatilised chlorides. This selective chlorination process^{3,8} would result in the pitting of the ferrochromium surface to a variable depth, since the chlorination products of iron silicide would be transported away from the site of the reaction and a network of chromium chlorides and carbon would remain (Fig. 10). An examination of the reaction surface by SEM served to confirm this mechanism (Fig. 11). From this it was concluded that the presence of free carbon and the carbide phase had had no obvious catalytic effect on the rate of reaction.

The chlorination of the carbide phase, in particular, led to the formation of a hard inner layer adjacent to the reaction interface. The layer was composed of unvolatilized chromium chlorides and minute traces of iron chlorides, trapped in a graphite matrix (Table II). High temperatures and high chlorine concentrations promoted thin inner layers of ash, which shows that the thickness of the layer was determined by an equilibrium between the rate of transport of the metallic chloride vapours from the layer and the rate of formation of new chlorides at the reaction interface. The mineralogical identification of the phases comprising the inner layer was made difficult by the numerous alteration products formed by the chloride species when the samples were removed from the reaction environment for analysis. The major alteration products were identified (by XRD analysis) as Cr_2O_3 , $\text{CrCl}_3 \cdot 6\text{H}_2\text{O}$, and CrOCl (from chromic chloride⁶), and $\text{FeCl}_2 \cdot 2\text{H}_2\text{O}$ and $\text{FeCl}_2 \cdot 4\text{H}_2\text{O}$, which were possibly alteration products of ferrous chloride.

Examination by SEM showed that chromic chloride appeared to be

the dominant chloride constituent of the inner layer at the reaction temperature, although some chromous chloride was identified by EDS (Fig. 12), and traces of ferrous chloride were identified by XRD. Most of the chromous chloride was in immediate contact with the reaction interface under the bulk inner layer (zone III). Reinhold and Hauffe⁹ identified a similar inner layer of chromous chloride among products of the chlorination of pure chromium metal. The existence of the thin layer of chromous chloride is explained by the thermodynamic data, since chromous chloride is a more stable reaction product than chromic chloride and ferrous chloride (Table IV).

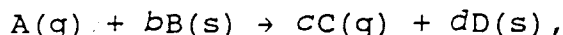
As chlorination proceeded, the inner ash layer (zone III) receded with the unreacted shrinking core of ferrochromium, leaving an outer layer of product ash at a sharply defined interface. XRD and chemical analysis (Table II), showed that the outer layer of product ash consisted essentially of an inert graphite matrix containing very few product chlorides and some unchlorinated cristobalite and fayalite. The presence of cristobalite and fayalite (which were present in the original sintered pellet) would be expected, since silica is relatively 'inert' to chlorine gas. Similarly, the slight concentration of calcium and magnesium was not surprising, because both elements form liquid dichloride species with low vapour pressures at typical reaction temperatures. Also, Robinson and Crosby¹⁰ claim that the presence of carbonaceous material (about 93 per cent by mass of the outer ash layer) further depresses the volatility of liquid dichlorides to below their thermodynamic vapour pressures.

The outer layer of product ash was porous to the reactant and product gases. The average pore diameter was 200 Å (determined by mercury porosimetry), and the density of the layer was 2.38 g cm⁻³. The layer retained the cylindrical shape and the dimensions (within 3 per cent) of the unchlorinated pellet, and was structurally bound to the unreacted shrinking core. As the reaction proceeded, the outer ash layer increased in thickness

until the completely reacted pellet was composed entirely of this material.

MATHEMATICAL MODELLING

The chlorination of a single particle of ferrochromium is a complex example of a topochemical, non-catalytic, heterogeneous reaction that exhibits USC behaviour. The general form of the reaction can be described by the equation



where the system is non-isothermal, involves an impure reactant that reacts to form two reaction interfaces, and is characterized by non-equimolar counter-diffusion.

The complex system was simplified as follows. Individual rate processes associated with the chlorination of ferrochromium (Fig. 13) were identified and, where reasonable, eliminated from the rate expression. Heat transfer by conduction within the pellet has already been shown to provide a negligible contribution to the overall rate of reaction, when compared to the contributions of convection and radiation away from the pellet, and can be disregarded accordingly. Furthermore, Themelis and Yannopoulos¹¹ claimed that, once the process temperature has been measured accurately, the kinetic data can be interpreted and correlated as a function of temperature without the mechanism of heat transfer being known. Consequently, the effects of heat transfer by convection and radiation were disregarded, thus further simplifying the mathematical treatment of the rate expression. At the temperature of operation of a chlorinator (935°C), the rate of sublimation of chromic chloride was shown to have only a minor effect on the overall rate of reaction, and so could be ignored.

It also appeared reasonable to neglect the contribution of the boundary-layer mass-transfer effects, since the tests were all carried out with gas velocities greater than the minimum critical

value. Furthermore, experimental evidence had strongly suggested that the overall rate of reaction was not controlled exclusively by the rate of the chemical reaction, and therefore, as a first approximation could be considered only in terms of the rate of diffusion through the layer of product ash.

Control by diffusion through the product ash

There is no exact analytical solution for the rate expression for diffusion through a growing layer of product ash on a short cylinder. Consequently, the short cylinder was considered to be an intermediate shape between the two geometrical extremes for which exact solutions exist, namely a sphere and an infinite cylinder. The fully chlorinated pellet of ferrochromium has external dimensions almost identical to those of the original pellet, so the simplified diffusion-control expressions were applicable, viz

$$1 - \frac{2}{3} X - (1-X)^{2/3} = k_{d,s}.t \quad (\text{for a sphere}), \text{ and}$$

$$X + (1-X) \ln (1-X) = k_{d,ic}.t \quad (\text{for an infinite cylinder}).$$

These expressions were plotted against reaction time for five data sets in the temperature range 900 to 975°C. Linear plots with correlation coefficients greater than 0.995 were generated, and these justified the approximation of the short-cylinder geometry by the two geometrical extremes, assuming exclusive control of the reaction by diffusion through the product ash layer. Arrhenius plots were therefore constructed so that approximate rate expressions for the chlorination of short cylinders of ferrochromium could be evaluated.

Arrhenius plots

The effect of temperature on the rate of reaction is normally evaluated by use of a modified form of the Arrhenius equation

$$\ln(k) = \ln(A_0) - E_A/RT$$

Plots of $\ln(k)$ against $1/T$ (Figs. 14 and 15) allowed the activation energies (- slope x R) and the frequency factors of the two diffusion processes to be calculated. Linear regressions were carried out only for data in the temperature range above 935°C, because below that temperature the rate of volatilisation of chromium chlorides is believed to have a significant effect on the overall rate of reaction. The following results were obtained.

Geometry	E_A , kJ mol ⁻¹	A_0 , min ⁻¹
Sphere	48.5	10.06
Infinite cylinder	42.6	17.85

The activation energies appear rather high, but an activation energy of 41.5kJ mol⁻¹ was claimed¹² for the reaction of zirconium tetrachloride with sodium chloride, the rate of which was also found to be 'controlled' by diffusion through the product ash layer. Although activation energies of this magnitude have been reported for Knudsen diffusion and bulk molecular diffusion¹³, the sheer magnitude of the values obtained in the present investigation would appear to exclude activated diffusion in a crystal lattice as the dominant diffusion mechanism. Also, the amount of impurities (especially carbon) present in the inner ash layer, made the migration of electronic defects an unlikely rate-limiting step.

Knudsen diffusion is likely to predominate over bulk molecular diffusion through the outer layer of product ash because the mean pore size is small (200 Å) compared to the mean free path calculated for the reactant gas (4272 Å). The presence of solid and fused chlorides in the inner ash layer is likely to impede diffusion processes through this layer to a greater degree than through the outer ash layer. Also, the molecular sizes of the

metal chloride vapours produced are larger than those of the reactant chlorine gas.

Hence, although reaction-rate constants have been evaluated for a general diffusion process, Knudsen diffusion of metal chloride vapours outwards through the inner ash layer appears to provide by far the largest single resistance to the overall rate of reaction. Consequently, it appears that the rate of chlorination of a single short cylinder of ferrochromium by a reactant gas containing a molar fraction of chlorine of 0.32, can be adequately approximated by the following expression:

$$1 - \sqrt[3]{X} - (1-X)^{2/3} = 10.06 \exp(-48.5 / 8.314 \times T)t$$

if the diffusion-control rate expression for a spherical sample is used.

CONCLUSIONS

The chlorination of short cylinders of sintered ferrochromium has been shown to proceed by a topochemical reaction. During the reaction, the samples exhibited unreacted shrinking-core behaviour, and partly reacted specimens had a multilayer structure consisting of an outer layer of graphitic ash, an inner layer of chromium chlorides, and an impervious ferrochromium core. The iron (chromium) silicide phases underwent chlorination and vapour transport more rapidly than did the chromium (iron) carbide phase.

At an initial reaction temperature of 800°C, the pellet developed a hard skin, which subsequently cracked, resulting in an enhanced rate of reaction. Between 850 and 900°C, the overall rate of reaction was independent of the temperature, and the rate of sublimation of chromium chlorides provided the major resistance to the overall rate of reaction. At temperatures above 935°C, diffusion through the layers of product ash, particularly Knudsen

diffusion of the product vapours through the inner layer of the product, is thought to provide the single largest resistance to the overall rate of reaction. The activation energy for the control of the rate of reaction by diffusion is between 42.6 and 48.5 kJ mol⁻¹.

ACKNOWLEDGEMENTS

This paper is published by permission of the Council for Mineral Technology (Mintek). Advice given by Dr N.A. Barcza, Mr T.R. Curr, and Ms K.C. Sole, assistance with the mineralogical investigations given by Mrs A. Wedepohl and Mr P. Ellis, and the help of Mr D.A.R. Duke and Mr C.K. Grassman with the experimental testwork, are gratefully acknowledged.

References

1. Badische Anilin - und Sodafabrik, British Patent no. 29235, 19th Dec 1913.
2. Edwards, A.M. A process for the production of metal value from a chromite product, South African Patent no.70/0222, 13th Jan. 1971, 11pp.
3. De Beauchamp, R.L. and Sullivan, T.A. Low-temperature chlorination of ferrochromium, U.S. Bureau of Mines Report of Investigations 7088, Mar. 1968, 8pp.
4. Dolganova, N.V., et al. 3. Methods for production of new types of raw materials for the manufacture of metallic chromium - Production of chromic chloride, Translated from Khimiya Tekhnologiya i,Primenenie Soedinenii Khrome i Sul'fidnykh Solei, 1975, p. 99-101.
5. Maier, C.G., Sponge Chromium, U.S. Bureau of Mines Bulletin no. 436, 1942, 109pp.

6. Nelson, L.R. Kinetics and mechanisms of the chlorination of ferrochromium, M.Sc. Dissertation, University of the Witwatersrand, 3rd Jun 1988, 261pp.
7. Gas-solid reactions, Szekely, J., Evans, J.W. and Sohn, H.Y., New York: Academic Press, 1976.
8. I.G. Farbenindustrie, A.G., A process for the production of iron-free chromium chloride from ferrochrome, Translated from German Patent no. 514 571, 4th Dec. 1930, 3pp.
9. Reinhold, K. and Hauffe, K. High temperature corrosion of chromium and chromium (III) oxide in chlorine and chlorine-oxygen mixtures, Journal of the Electrochemical Society, vol. 124, no. 6, June 1977, p. 875-883.
10. Robinson, M. and Crosby, A.D., Production of metal chlorides, European Patent no. 0 096 241, 14th May 1983, 25pp.
11. Themelis, N.J., and Yannopoulos, J.C. Mass- and heat-transfer phenomena in the reduction of cupric oxide by hydrogen. Transactions of The Metallurgical Society of AIME, vol. 236, April 1966, p. 414-420.
12. Majumdar, S., et al. Kinetics of reaction of zirconium tetrachloride vapors with solid sodium chloride spheres, Metallurgical Transactions B, vol. 6B, Dec. 1975, p. 607-612.
13. Miriyala, V.R.R., and Bowen, J.H. The reduction of ferrous chloride with hydrogen, Canadian Journal of Chemical Engineering, vol. 49, Dec. 1971, p. 804-809.

Table I Thermodynamic data for reactions that take place during the production of chromium chlorides

Reaction no.	Reaction	ΔH_{1000}° °C kJ mol ⁻¹ *	ΔG_{1000}° °C kJ mol ⁻¹ *
<i>Chromium chlorination</i>			
1	$\text{Cr(s)} + \text{Cl}_2(\text{g}) \rightarrow \text{CrCl}_2(\text{l})$	-280.5	-245.1
2	$\frac{2}{3}\text{Cr(s)} + \text{Cl}_2(\text{g}) \rightarrow \frac{2}{3}\text{CrCl}_3(\text{g})$	-142.6	-188.8
3	$\frac{1}{2}\text{Cr(s)} + \text{Cl}_2(\text{g}) \rightarrow \frac{1}{2}\text{CrCl}_4(\text{g})$	-162.2	-146.6
4	$\frac{2}{21}\text{Cr}_7\text{C}_3(\text{s}) + \text{Cl}_2(\text{g}) \rightarrow \frac{2}{3}\text{CrCl}_3(\text{g}) + \frac{2}{7}\text{C(s)}$	-120.3	-167.4
5	$\frac{1}{14}\text{Cr}_7\text{C}_3(\text{s}) + \text{Cl}_2(\text{g}) \rightarrow \frac{1}{2}\text{CrCl}_4(\text{g}) + \frac{3}{14}\text{C(s)}$	-145.4	-130.6
<i>Chromic oxide chlorination</i>			
6	$\frac{1}{3}\text{Cr}_2\text{O}_3(\text{s}) + \text{Cl}_2(\text{g}) \rightarrow \frac{2}{3}\text{CrCl}_3(\text{g}) + \frac{1}{2}\text{O}_2(\text{g})$	+249.9	+76.2
7	$\frac{1}{4}\text{Cr}_2\text{O}_3(\text{s}) + \text{Cl}_2(\text{g}) \rightarrow \frac{1}{2}\text{CrCl}_4(\text{g}) + \frac{3}{8}\text{O}_2(\text{g})$	+132.2	+52.1
8	$\frac{1}{3}\text{Cr}_2\text{O}_3(\text{s}) + \frac{1}{2}\text{C(s)} + \text{Cl}_2(\text{g}) \rightarrow \frac{2}{3}\text{CrCl}_3(\text{g}) + \frac{1}{2}\text{CO}_2(\text{g})$	+61.1	-122.7
9	$\frac{1}{4}\text{Cr}_2\text{O}_3(\text{s}) + \frac{3}{8}\text{C(s)} + \text{Cl}_2(\text{g}) \rightarrow \frac{1}{2}\text{CrCl}_4(\text{g}) + \frac{3}{8}\text{CO}_2(\text{g})$	-9.5	-97.1
<i>Chlorination by FeCl₃(g)</i>			
10	$\frac{2}{3}\text{Cr(s)} + \frac{2}{3}\text{FeCl}_3(\text{g}) \rightarrow \frac{2}{3}\text{CrCl}_3(\text{g}) + \frac{2}{3}\text{Fe(s)}$	+149.0	-39.2
11	$\text{CrCl}_2(\text{s}) + \text{FeCl}_3(\text{g}) \rightarrow \text{CrCl}_3(\text{s}) + \text{FeCl}_2(\text{l})$	+492.7	-15.3
<i>Iron chlorination</i>			
12	$\text{Fe(s)} + \text{Cl}_2(\text{g}) \rightarrow \text{FeCl}_2$	-88.2	-201.6
13	$\frac{2}{3}\text{Fe(s)} + \text{Cl}_2(\text{g}) \rightarrow \frac{2}{3}\text{FeCl}_3(\text{g})$	-115.6	-149.6
14	$\frac{2}{3}\text{Fe(s)} + \text{Cl}_2(\text{g}) \rightarrow \frac{1}{3}\text{Fe}_2\text{Cl}_6(\text{g})$	-159.4	-139.9
15	$\frac{2}{13}\text{Fe}_3\text{Si(s)} + \text{Cl}_2(\text{g}) \rightarrow \frac{6}{13}\text{FeCl}_3(\text{g}) + \frac{2}{13}\text{SiCl}_4(\text{g})$	-151.2	-163.5
<i>Silicon chlorination</i>			
16	$\frac{1}{2}\text{Si(s)} + \text{Cl}_2(\text{g}) \rightarrow \frac{1}{2}\text{SiCl}_4$	-278.0	-244.1
<i>Disproportionation reactions</i>			
17	$2\text{CrCl}_4(\text{g}) \rightarrow 2\text{CrCl}_3(\text{g}) + \text{Cl}_2(\text{g})$	+462.3	+20.1
18	$2\text{CrCl}_3(\text{g}) \rightarrow 2\text{CrCl}_2(\text{l}) + \text{Cl}_2(\text{g})$	+588.5	+76.2
19	$2\text{CrCl}_3(\text{g}) \rightarrow \text{CrCl}_4(\text{g}) + \text{CrCl}_2(\text{l})$	+508.0	+28.0
20	$2\text{FeCl}_3(\text{g}) \rightarrow 2\text{FeCl}_2(\text{l}) + \text{Cl}_2(\text{g})$	+659.2	+45.7
21	$\text{Fe}_2\text{Cl}_6(\text{g}) \rightarrow 2\text{FeCl}_2(\text{l}) + \text{Cl}_2(\text{g})$	+514.7	+16.5

*kJ per mole of chlorine gas

Table II Typical chemical analyses (expressed as per cent by mass)

Material	Cr	Fe	C	Si	Ti	Ni	Ca	Mg	Cl	Cr/ Fe	Total
Charge- chrome fines	52.7	35.9	6.5	3.18	0.35	0.15	0.14	0.04	n.a	1.4	99.4*
Outer ash layer	0.2	<0.2	93.8	1.23	0.11	0.01	0.25	0.05	0.4	>1	95.8
Inner ash layer	20.6	<0.2	32.0	0.84	0.11	0.34	0.08	0.07	17.9	>103	71.9
Unreacted shrinking core	50.1	36.2	6.4	4.23	0.41	0.29	0.20	<0.1	0.07	1.4	96.2

* The charge-chrome also contained the following minor and trace elements:

V 0.28% O 0.08%
Mn 0.19% S 0.03%
Co 0.02% P 0.024%

n.a Not applicable

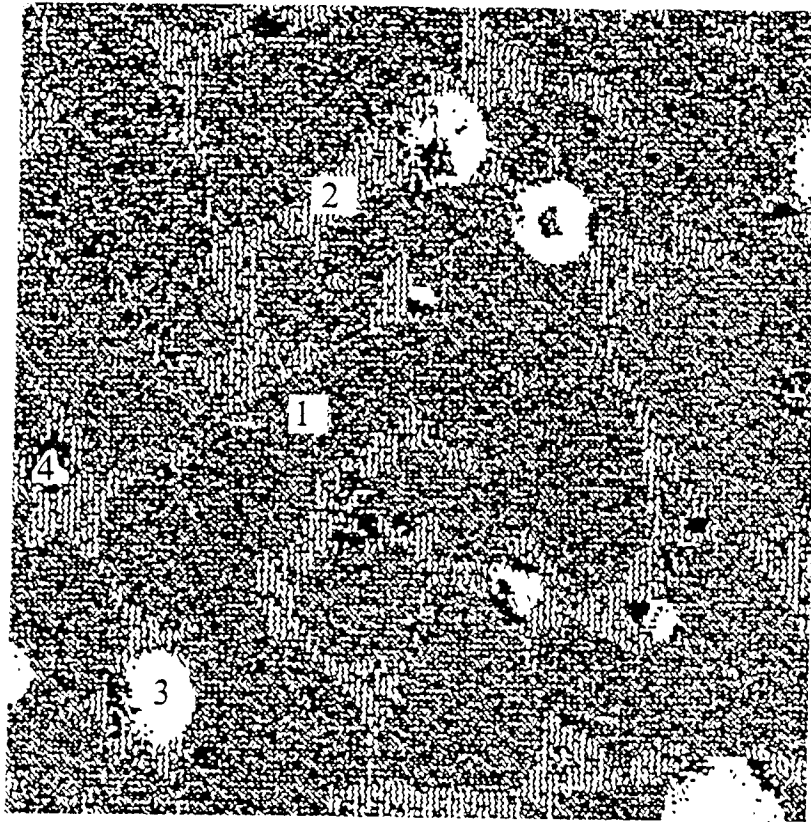
TABLE III Comparison of the initial rates of chlorination of ferrochromium and the rate of sublimation of chromic chloride

	$T, ^\circ\text{C}$	Rate* , g s^{-1}
CrCl ₃ Pellet	858	0.095
	931	0.184
FeCr Pellet	850	0.109
	925	0.115

* The rate, given by the expression $\frac{d\Delta m_{\text{Cr}}}{dt}$, is expressed per unit surface area.

TABLE IV Standard free energies of formation of metal chlorides and their thermodynamic equilibrium partial pressures of chlorine gas at 900°C^6

Species	$\Delta G^0_{900^\circ\text{C}}, \text{kJ}$	$p_{\text{Cl}_2(\text{g})}, \text{atmospheres}$ per mole of chlorine gas
Ferrous chloride (FeCl ₂)	- 197.03	1.68×10^{-9}
Chromium chloride (CrCl ₃)	- 195.98	1.87×10^{-9}
Chromous chloride (CrCl ₂)	- 253.19	5.3×10^{-12}



256 by 256 X-ray map
Magnification 400x

100 μm

Material	Area
1 (Cr,Fe) ₇ C ₃	76%
2 (Fe,Cr) ₃ Si	17%
3 Pores	7%
4 Slag inclusion	5%

Fig. 2 X-ray map of a sectioned sintered pellet

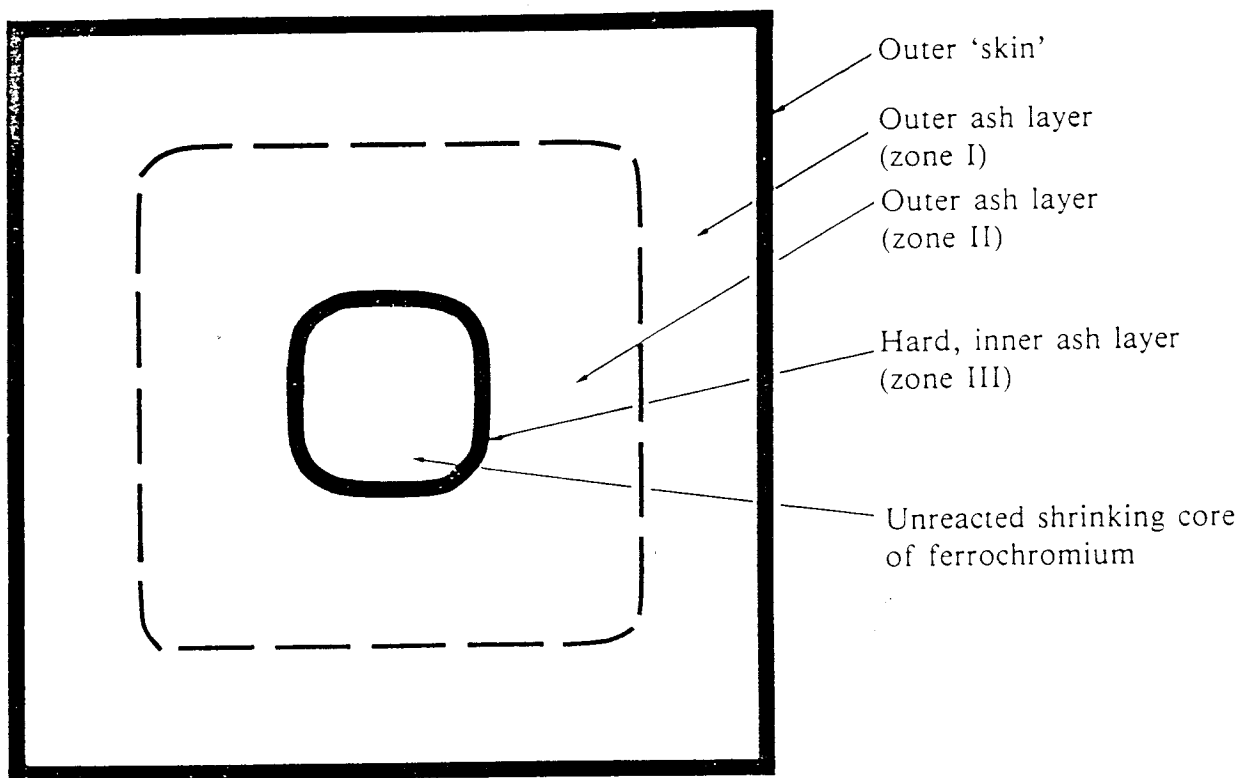


Fig. 4 Schematic diagram of the various layers of reaction products

502 Nelson
Date 2/3/52

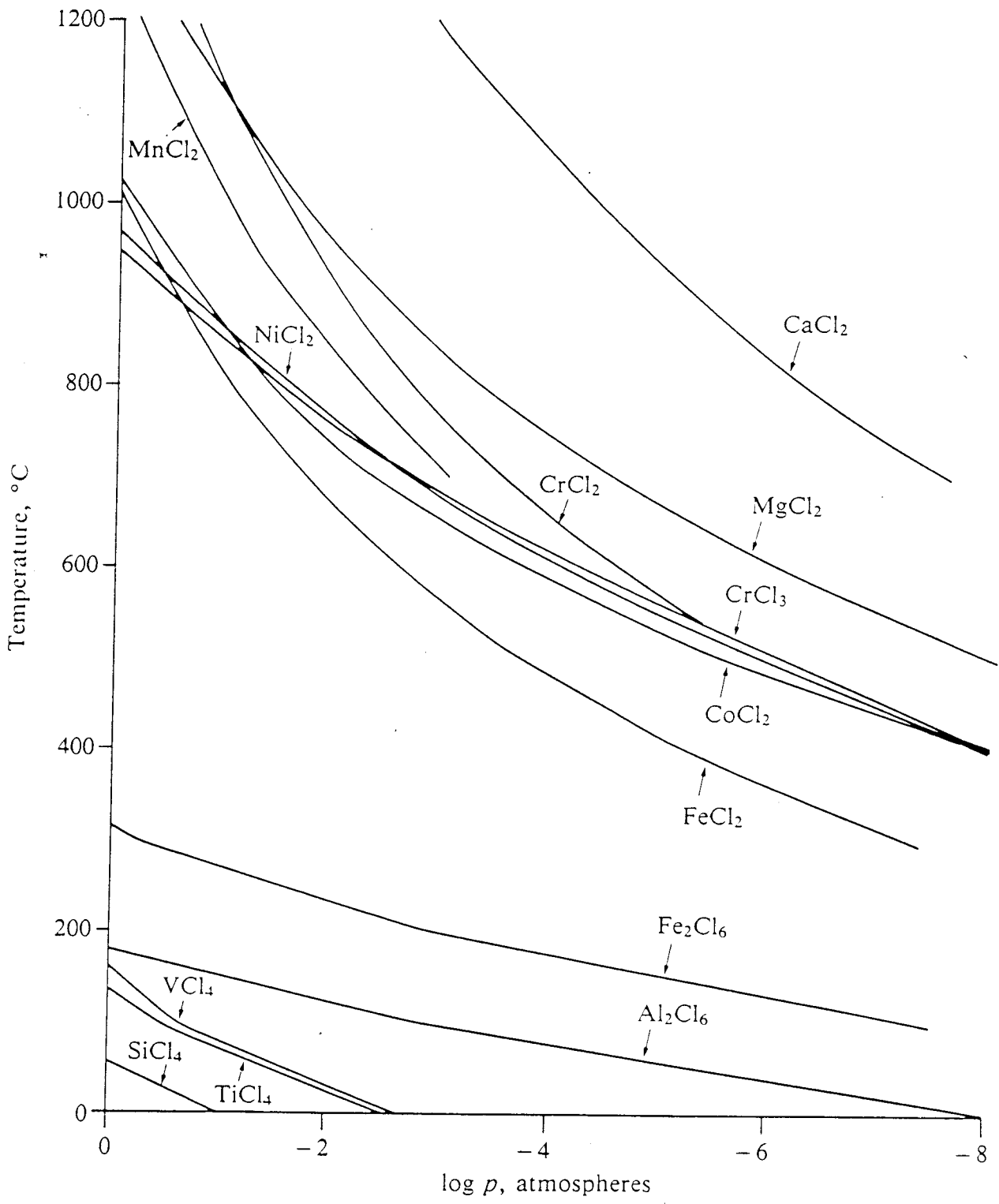


Fig. 1 Effect of temperature on the vapour pressure of metal chlorides

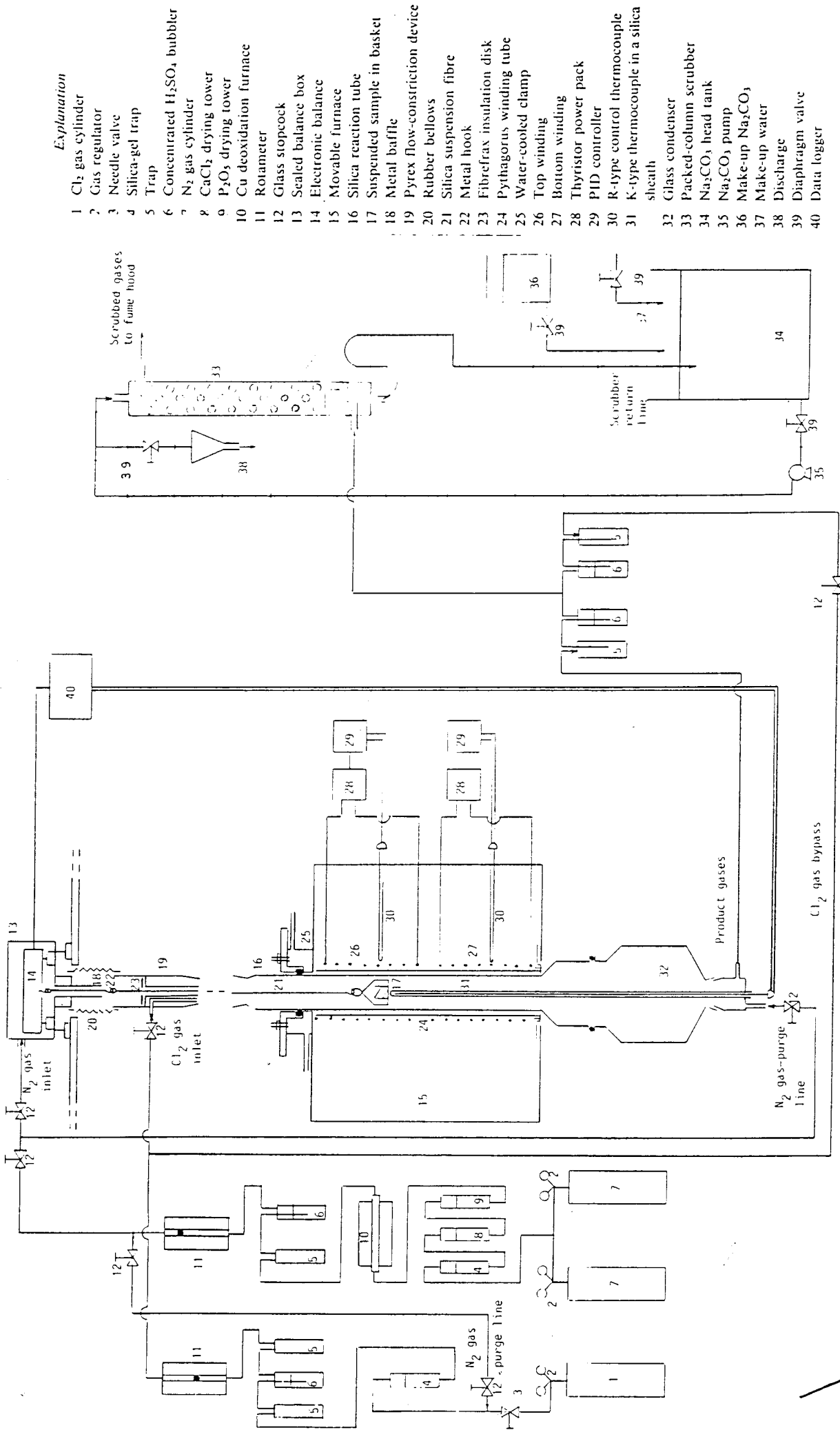


Fig. 3 Apparatus used for the chlorination of ferrochromium

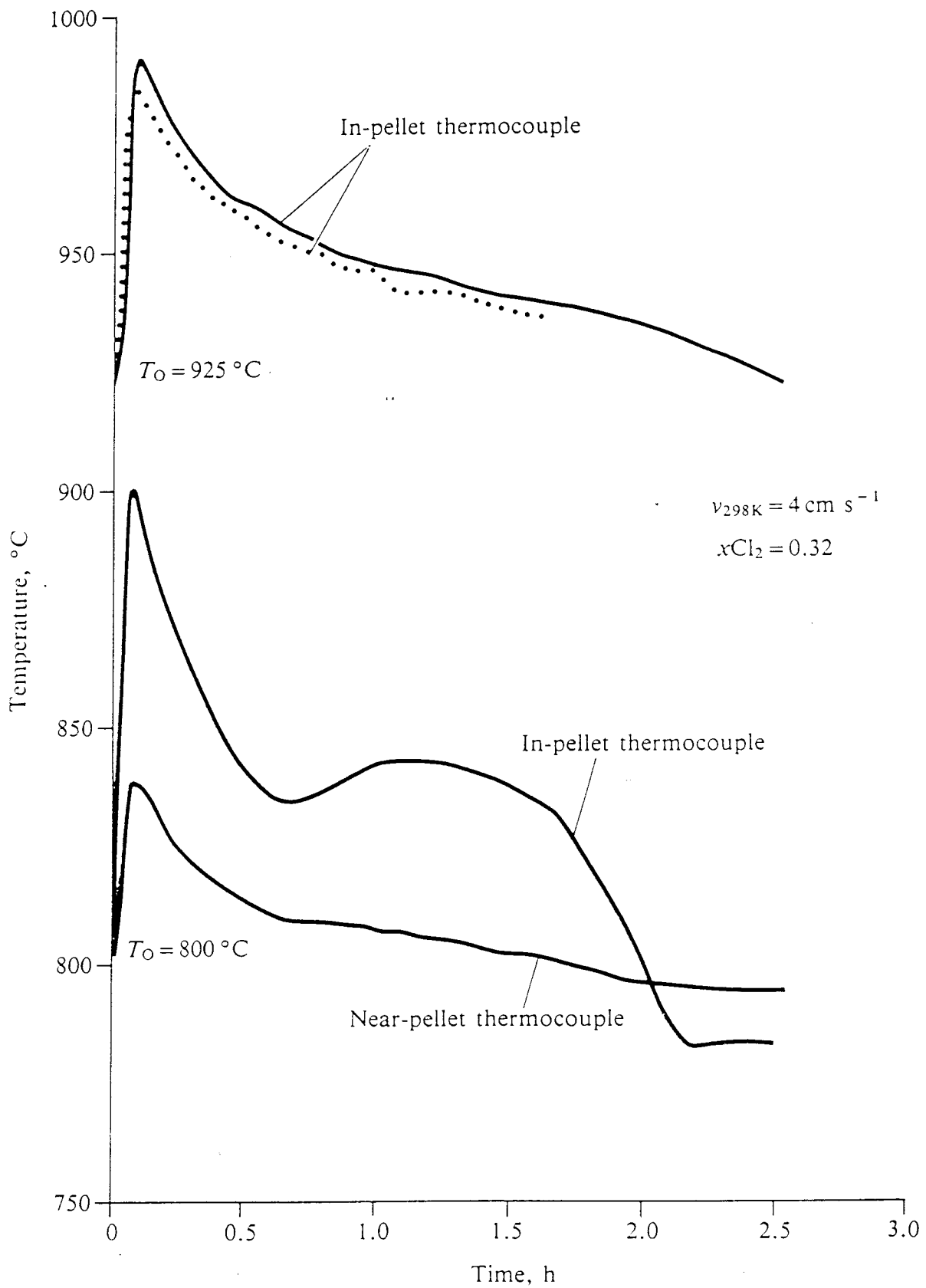


Fig. 5 Temperature changes in and near the pellet during chlorination

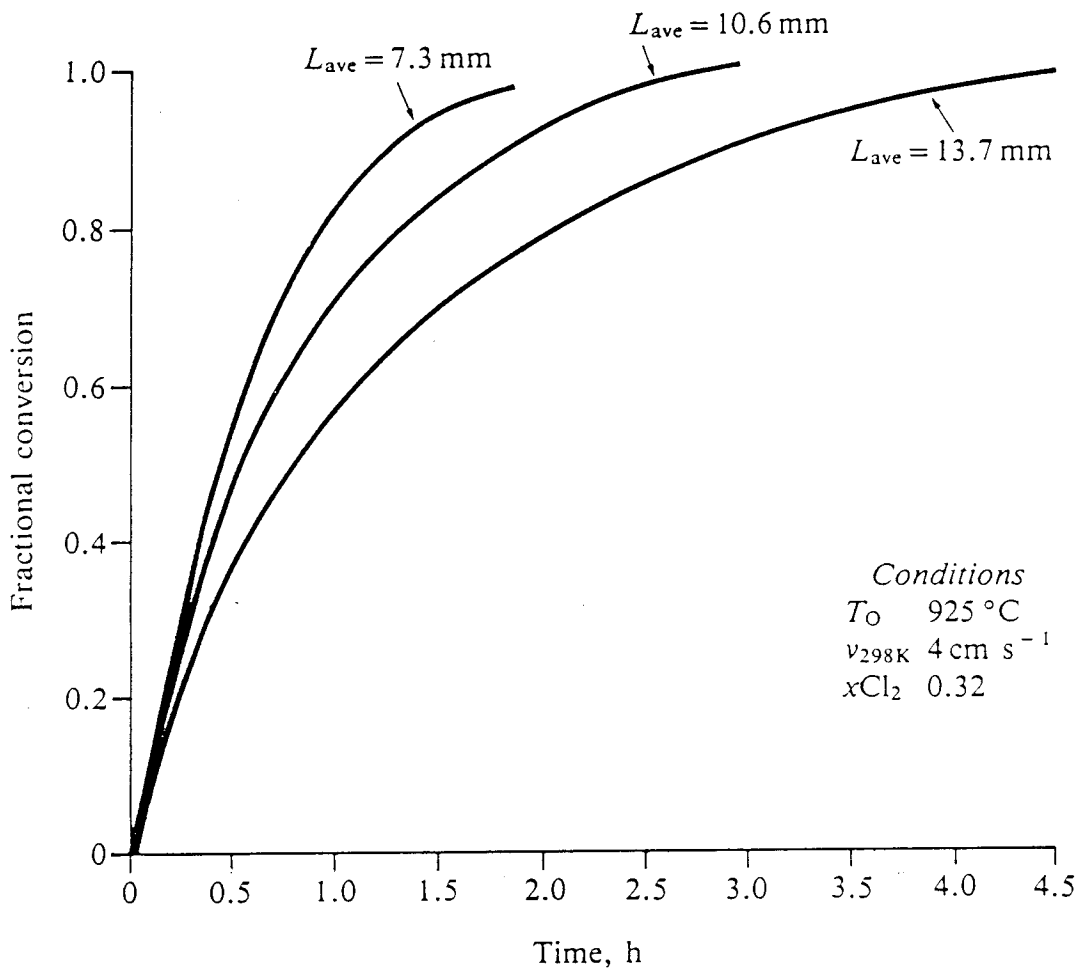


Fig. 6 Effect of pellet size on the rate of reaction

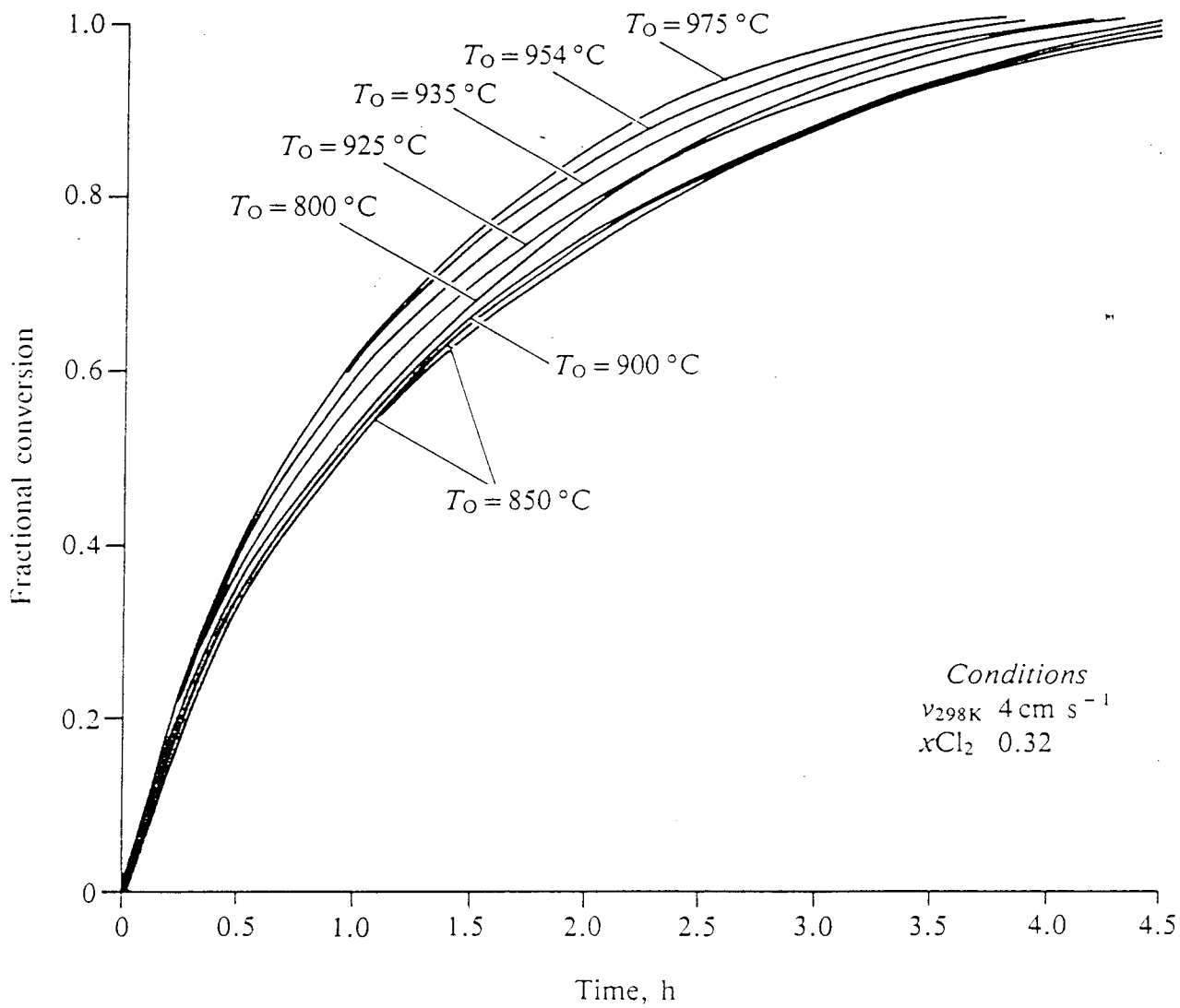


Fig. 7 Effect of initial reaction temperature on the rate of reaction

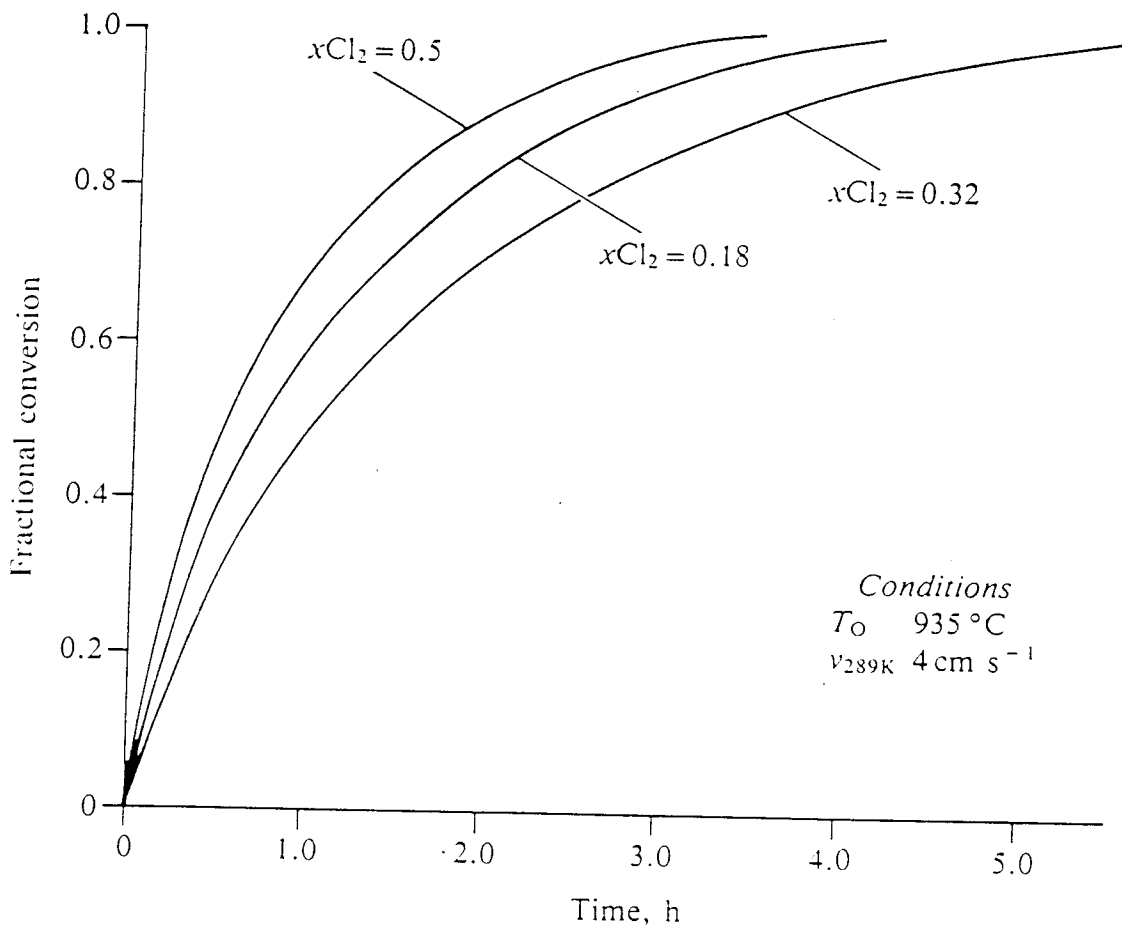


Fig. 8 Effect of chlorine concentration on the rate of reaction

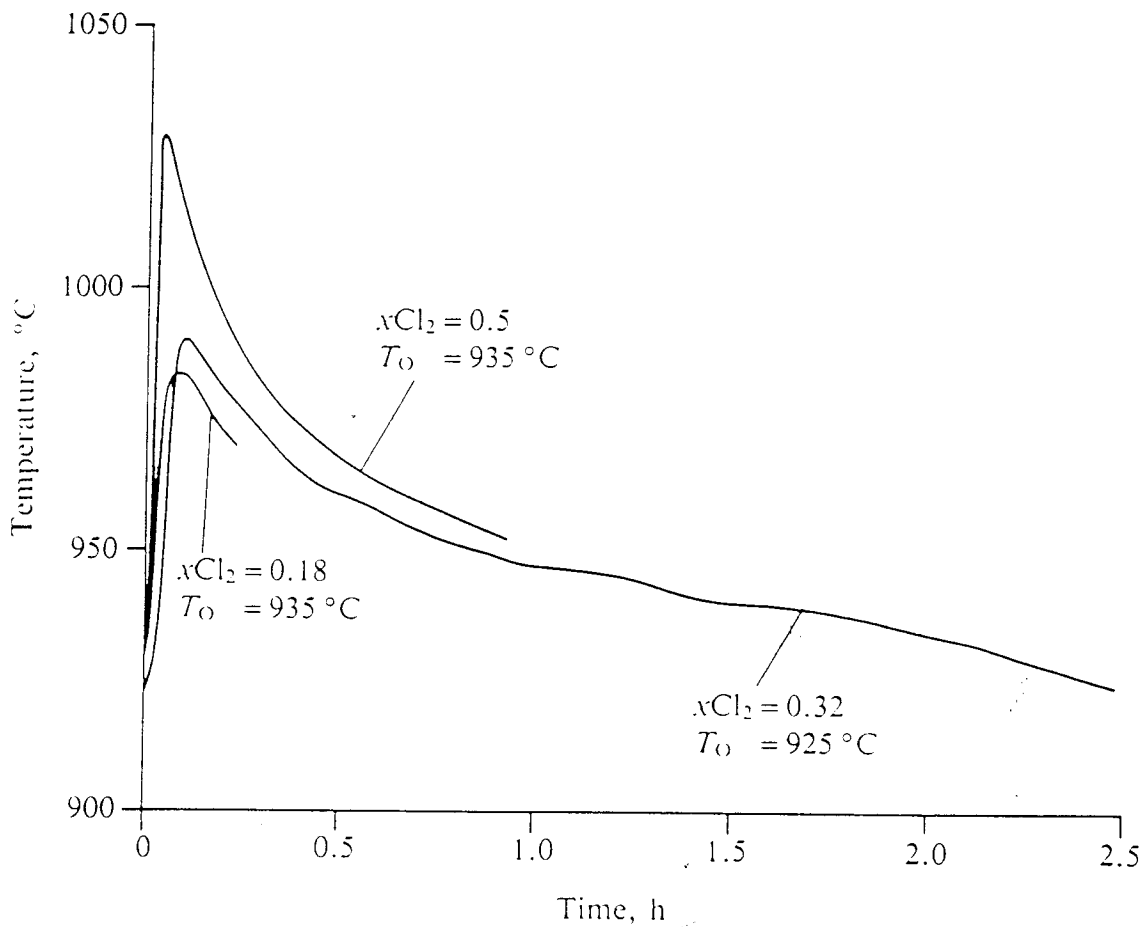


Fig. 9 Effect of chlorine concentration on the temperature within the pellet







- 1 Cr_7C_3 in pit
- 2 Cr_2O_3

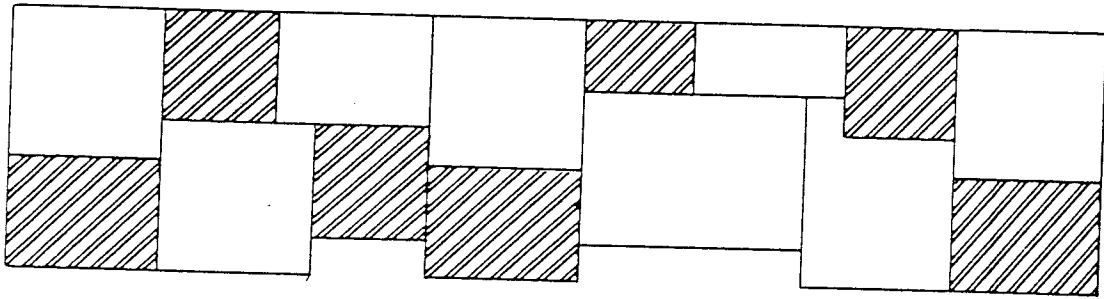


- 1 Cr_7C_3 in pit
- 2 CrCl_2
- 3 CrOCl

Fig. 11 Photomicrographs (by SEM) of the reaction interface

-  Cr_7C_3
-  Fe_3Si
-  Mixed chromium chlorides and graphite
-  CrCl_2 at the reaction interface

Before chlorination



Partly chlorinated

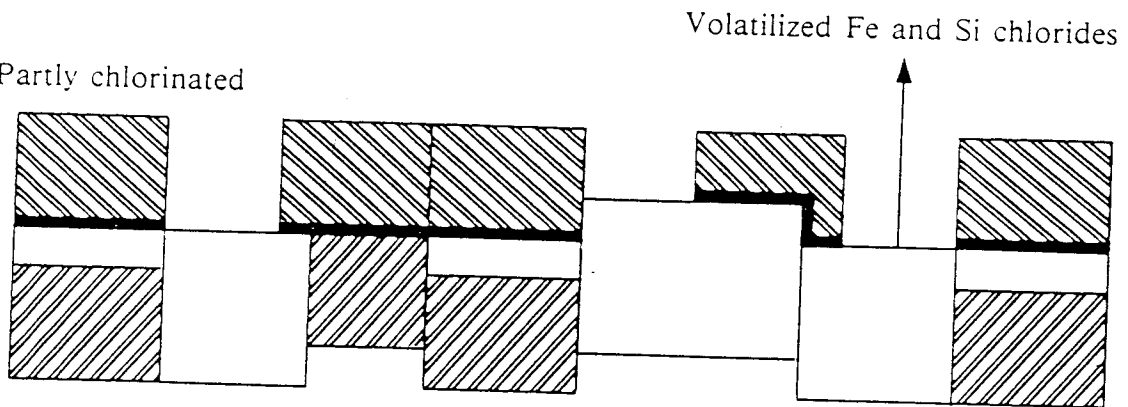


Fig. 10 Schematic diagram of the reaction mechanism

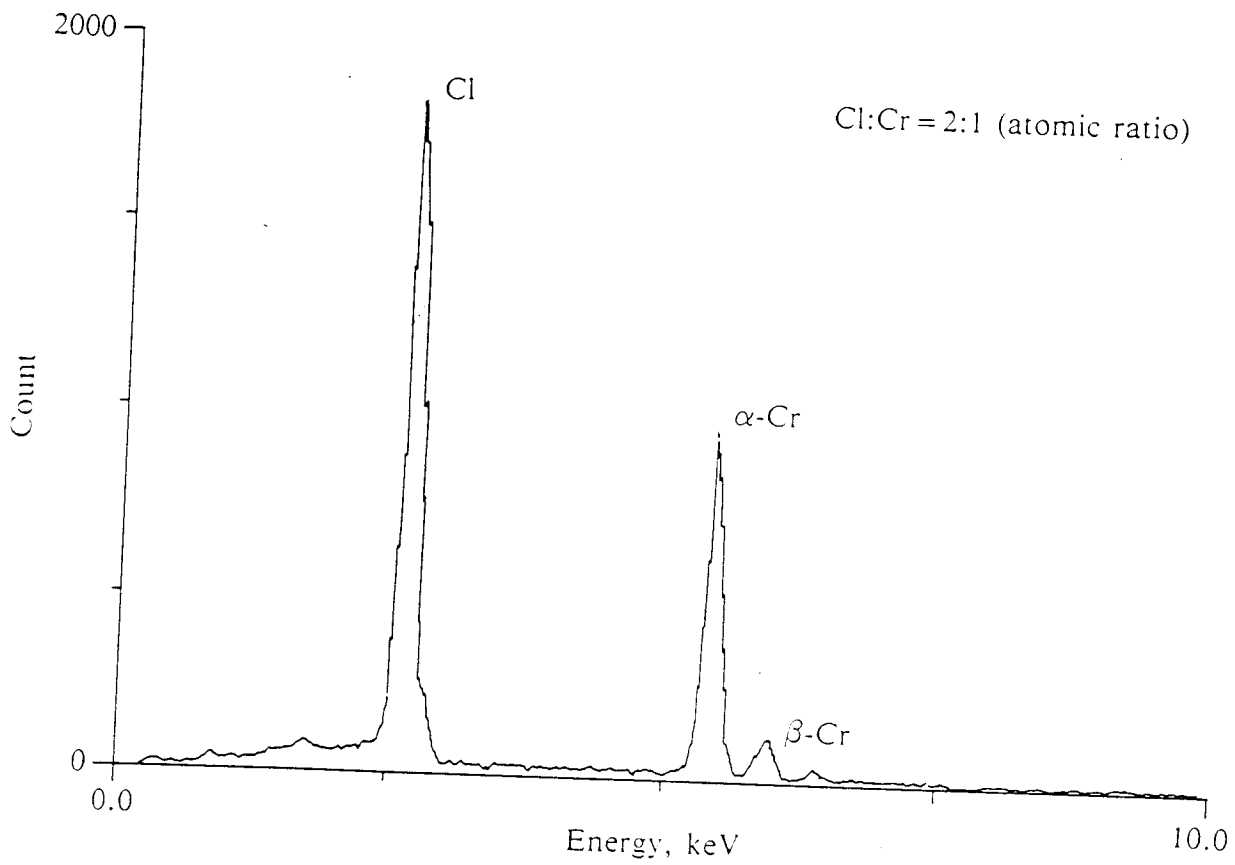
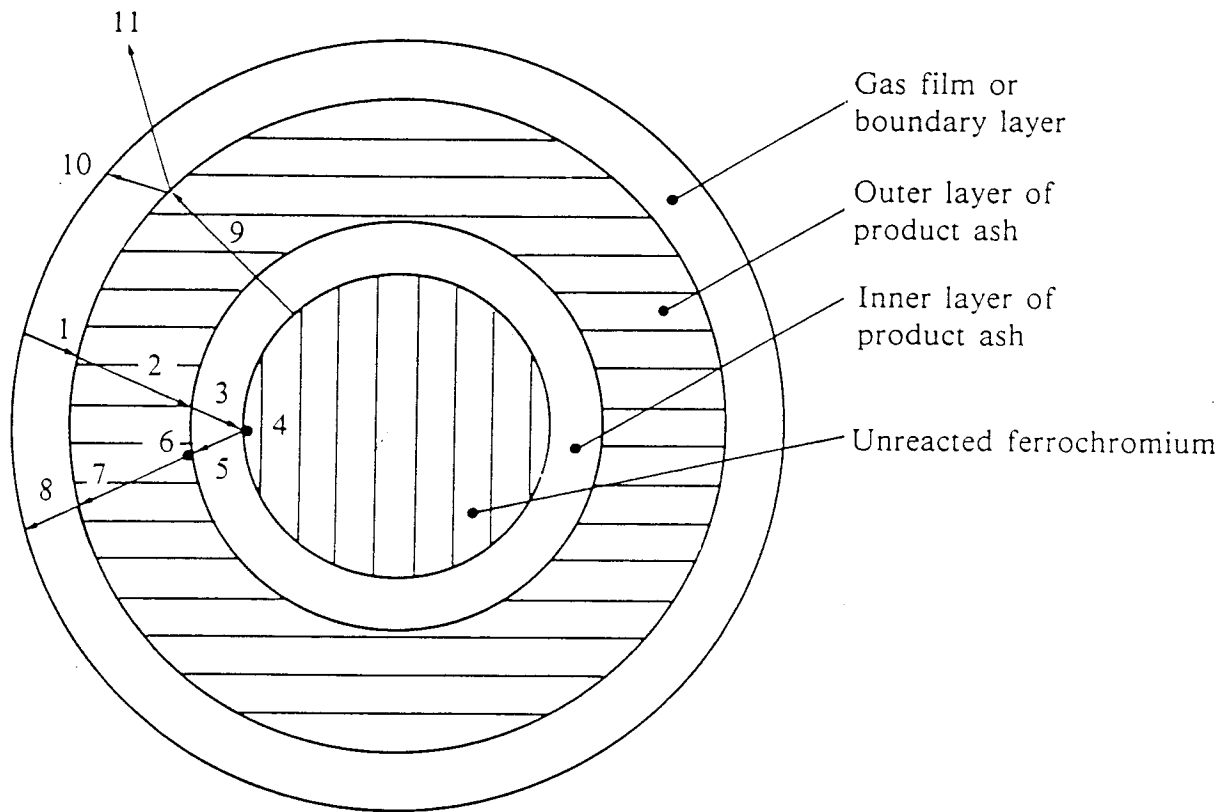


Fig. 12 Analysis of CrCl_2 (point 2 in Fig. 11b) by EDS



- 1 Mass transfer of chlorine gas across boundary layer
- 2 Diffusion of chlorine gas through outer product layer
- 3 Diffusion of chlorine gas through inner product layer
- 4 Chemical reaction at non-porous ferrochromium surface
- 5 Diffusion of product chloride gases through inner product layer
- 6 Vaporization of chromium chlorides from inner product layer
- 7 Diffusion of product chloride gases through outer product layer
- 8 Mass transfer of product chloride gases across boundary layer
- 9 Heat transfer through pellet by conduction
- 10 Heat transfer across boundary layer by convection
- 11 Heat transfer across boundary layer by radiation

Fig. 13 Schematic diagram of the rate processes involved in the chlorination of ferrochromium

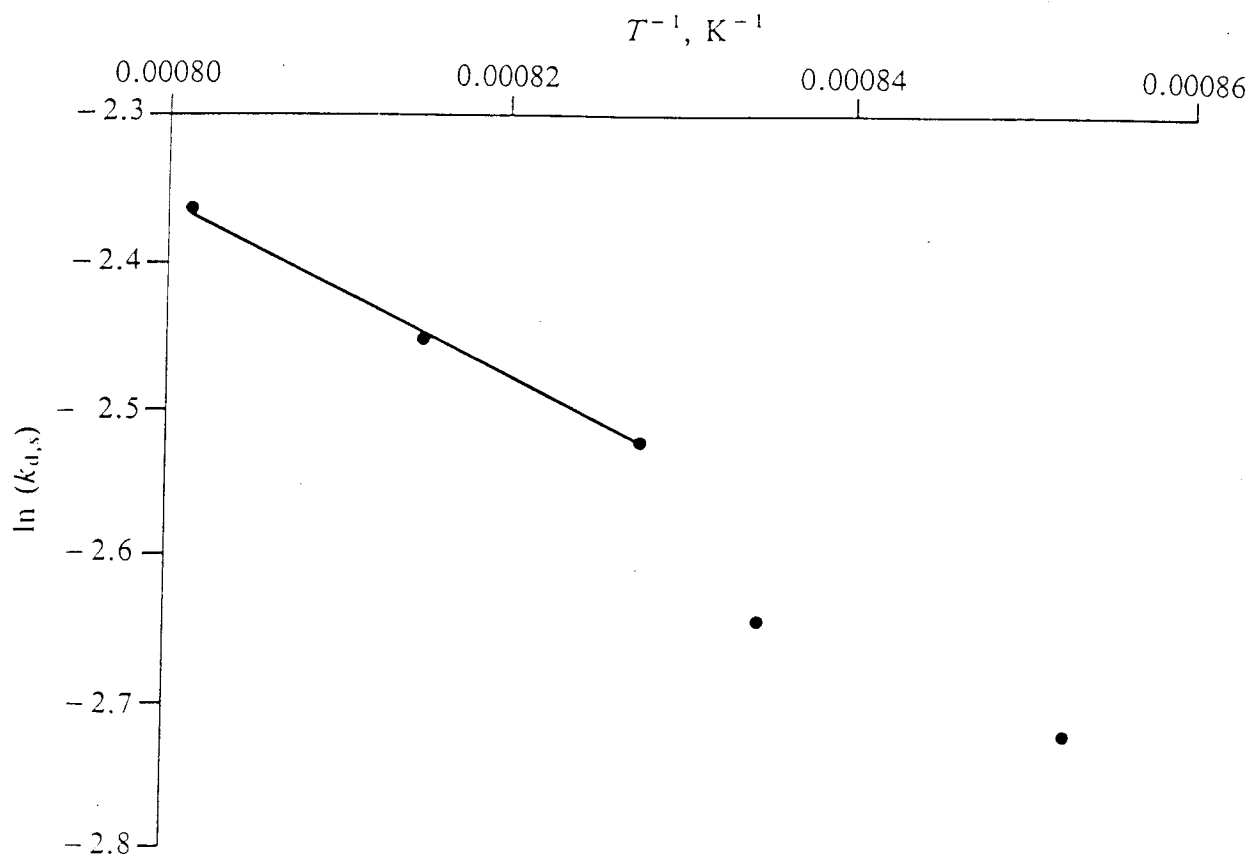


Fig. 14 Arrhenius plot for a spherical geometry

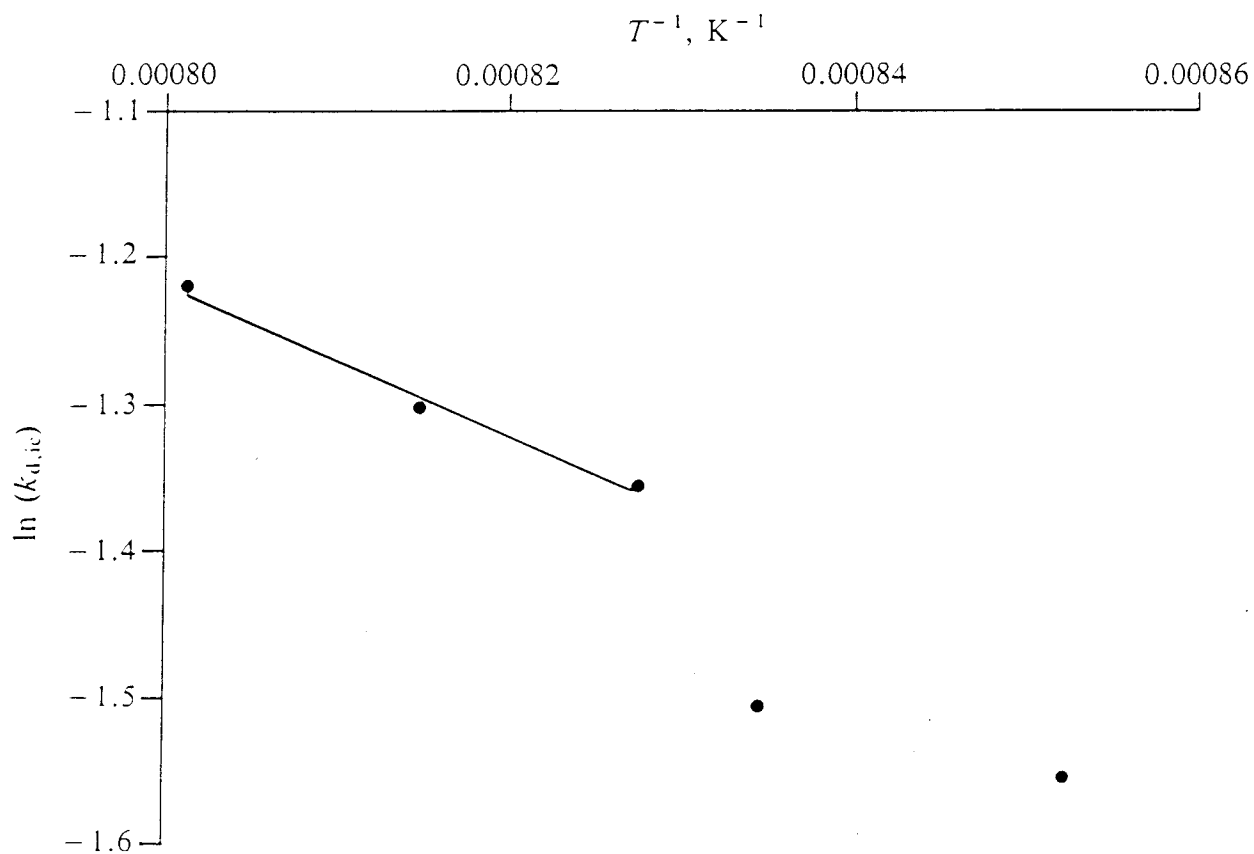


Fig. 15 Arrhenius plot for a cylindrical geometry